Surface Science 649 (2016) 14–19

Contents lists available at ScienceDirect

Surface Science

journal homepage: www.elsevier.com/locate/susc

# Low-temperature one-atom-layer $\sqrt{7} \times \sqrt{7}$-In phase on Si(111)

A.N. Mihalyuk [a,b], A.A. Alekseev [a], C.R. Hsing [c], C.M. Wei [c], D.V. Gruznev [a,b], L.V. Bondarenko [a,b], A.V. Matetskiy [a,b], A.Y. Tupchaya [a,b], A.V. Zotov [a,b,d], A.A. Saranin [a,b,*]

[a] Institute of Automation and Control Processes FEB RAS, 5 Radio Street, 690041 Vladivostok, Russia
[b] School of Natural Sciences, Far Eastern Federal University, 690950 Vladivostok, Russia
[c] Institute of Atomic and Molecular Sciences, Academia Sinica, P.O. Box 23-166, Taipei, Taiwan
[d] Department of Electronics, Vladivostok State University of Economics and Service, 690600 Vladivostok, Russia

ARTICLE INFO

*Article history:*
Received 28 October 2015
Accepted 20 January 2016
Available online 28 January 2016

*Keywords:*
Atom–solid interactions
Silicon
Indium
Ab initio random structure searching
Scanning tunneling microscopy
Low energy electron diffraction

ABSTRACT

The Si(111)-hex-$\sqrt{7} \times \sqrt{3}$-In reconstruction has been attracted considerable attention due to its superconducting properties occurring in the one-atom-layer metal film. However, the $\sqrt{7} \times \sqrt{3}$ periodicity is a characteristic feature of this surface only at room temperature. Upon cooling to low temperatures the $\sqrt{7} \times \sqrt{3}$ structure transforms reversibly to the $\sqrt{7} \times \sqrt{7}$ one that should not be ignored while considering superconductivity in this system. In the present study, atomic structure of the low-temperature one-atom-layer Si(111)$\sqrt{7} \times \sqrt{7}$-In phase has been evaluated using scanning tunneling microscopy (STM), low-energy electron diffraction (LEED) and ab initio random structure searching (AIRSS) technique. Basing on the LEED observations, it has been found that the $\sqrt{7} \times \sqrt{7}$-In surface incorporates plausibly eight In atoms per $\sqrt{7} \times \sqrt{7}$ unit cell (i.e., ~1.14 ML In). AIRSS demonstrates occurrence of a set of various surface structures with very close formation energies. Some of their counterparts can be found in the experimental STM images.



## 1. Introduction

Seminal discovery of a superconductivity in the In/Si(111) and Pb/Si(111) reconstructions [1,2,3] demonstrated that a superconductor can be confined down to the one-atom-layer thickness. This discovery stimulated the researches directed towards understanding peculiarities of superconductivity at the ultimate atomic limit (e.g., character of electron–phonon coupling [4,5,6] and effects of structural disorder [7]). The highest temperature of the superconducting transition was found in the quasi-rectangular rec-$\sqrt{7} \times \sqrt{3}$-In phase where it amounts to ~3.0 K [1,2,3] (the value close to that in bulk In). This was initially thought as an inherent property of one-atom-layer thick In film, because to that moment it was commonly accepted that the rec-$\sqrt{7} \times \sqrt{3}$ phase is essentially an In(100) atomic layer (having 1.2 ML In coverage) atop a bulk-like Si(111) surface. [One monolayer (ML) = $7.8 \times 10^{14}$ cm$^{-2}$, the top Si atom density in unreconstructed Si(111)1 × 1 surface.] Meanwhile, the other $\sqrt{7} \times \sqrt{3}$ phase called quasi-hexagonal hex-$\sqrt{7} \times \sqrt{3}$ was considered to be a pseudomorphic In/Si(111) layer having 1.0 ML In coverage [8]. However, composition of the $\sqrt{7} \times \sqrt{3}$ phases has recently been reconsidered and their new structural models have been proposed [9,10]. It was concluded that the rec-$\sqrt{7} \times \sqrt{3}$ phase incorporates 2.4 ML In in the double atomic layer of In. Hence, strictly speaking, its advanced superconducting properties refer not to a single atomic layer but to the two In layers. Nevertheless, the hex-$\sqrt{7} \times \sqrt{3}$ (which was found to be actually the one-atom-layer phase with 1.2 ML In) also shows superconductivity, albeit at slightly lower temperature, 2.4 K [3]. The In coverage value of 1.2 ML established for hex-$\sqrt{7} \times \sqrt{3}$ allowed to propose an adequate structural model of 2 × 2-In phase (which can be thought as hex-$\sqrt{7} \times \sqrt{3}$ precursor) adopting 1 ML In [11,12]. However, the same finding erected a problem we would like to discuss in this paper. Namely, we found that upon cooling the hex-$\sqrt{7} \times \sqrt{3}$ undergoes a reversible phase transition to the hexagonal $\sqrt{7} \times \sqrt{7}$ structure [13]. The puzzling feature of this transition is that the low-temperature $\sqrt{7} \times \sqrt{7}$ surface phase cannot adopt exactly 1.2 ML In with integer number of In atoms per $\sqrt{7} \times \sqrt{7}$ unit cell. Another demand for determining an atomic structure of the $\sqrt{7} \times \sqrt{7}$ phase stems from the fact that while considering superconductivity of the hex-$\sqrt{7} \times \sqrt{3}$-In phase one has to take into account that its original (room-temperature) atomic structure is not preserved upon cooling to low temperatures.

The goal of the present study was to elucidate the atomic arrangement of the low-temperature Si(111)$\sqrt{7} \times \sqrt{7}$-In surface phase. We have found that the $\sqrt{7} \times \sqrt{7}$ phase incorporates slightly less In than the room-temperature hex-$\sqrt{7} \times \sqrt{3}$ with 1.2 ML In, namely, eight In

* Corresponding author at: Institute of Automation and Control Processes FEB RAS, 5 Radio Street, 690041 Vladivostok, Russia.
*E-mail address:* saranin@iacp.dvo.ru (A.A. Saranin).

http://dx.doi.org/10.1016/j.susc.2016.01.016
0039-6028/

atoms per $\sqrt{7} \times \sqrt{7}$ unit cell (i.e., ~1.14 ML In). Ab initio random structure searching generates a set of various structures having very close formation energies. Their counterparts, albeit not all, can be found in the experimental scanning tunneling microscopy images.

## 2. Experimental and calculation details

Our experiments were performed with Omicron MULTIPROBE system operated in an ultrahigh vacuum (~$2.5 \times 10^{-10}$ mbar). Atomically-clean Si(111)$7 \times 7$ surface was prepared in situ by flashing to 1280 °C after the sample was first outgassed at 600 °C for several hours. Indium was deposited from Ta crucible at a rate of 0.06 ML/min. The In/Si(111)$\sqrt{7} \times \sqrt{7}$ reconstructions were prepared by In deposition onto the In/Si(111)$\sqrt{3} \times \sqrt{3}$ surface held at RT. Structure of the forming In/Si(111) surfaces was monitored using LEED and STM observations.

Density functional theory calculations were performed using projector-augmented-wave method (PAW) [14,15], as implemented in Vienna Ab-initio Simulation Package (VASP) [16,17]. The exchange-correlation function was treated in the local density approximation (LDA) [18]. In order to find the most stable structures adopted by the $\sqrt{7} \times \sqrt{7}$-reconstructed In/Si(111) surface, we used ab initio

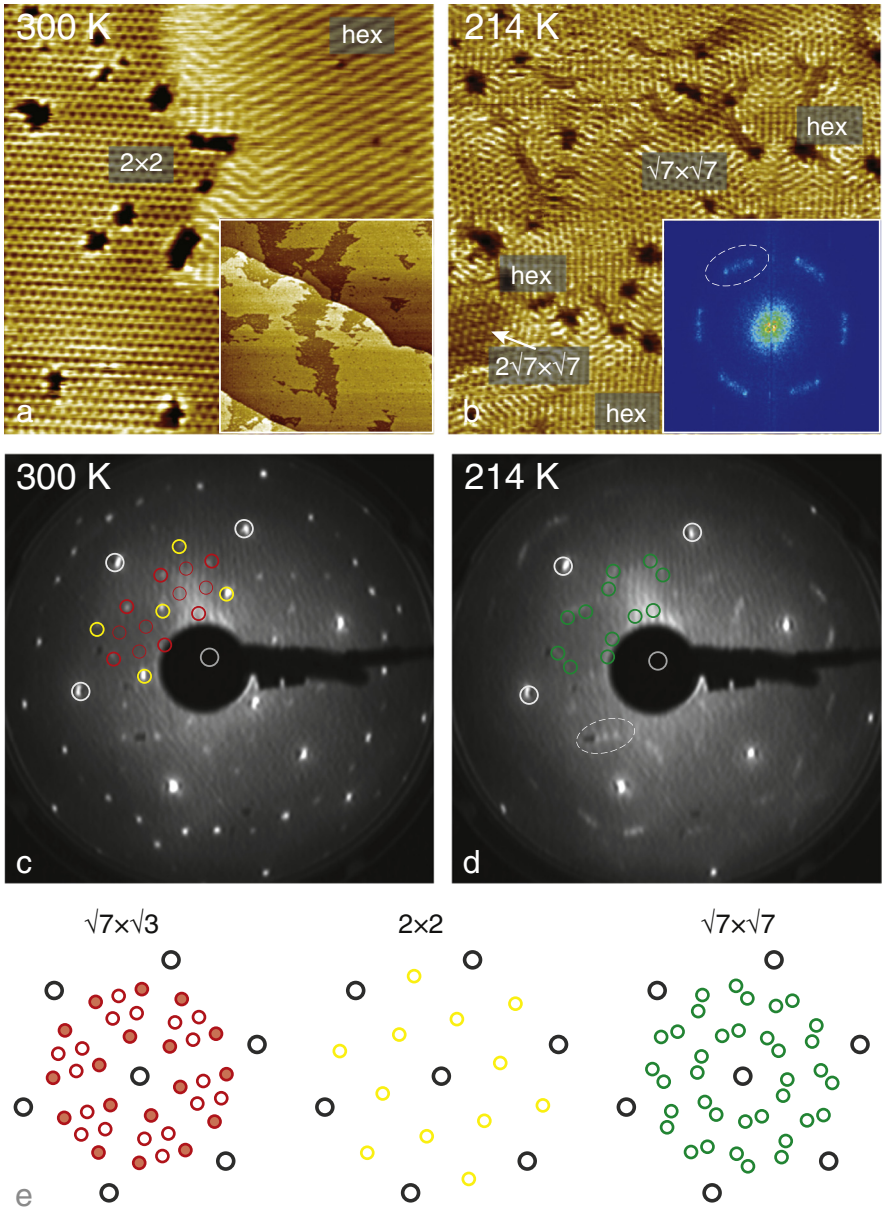


**Fig. 1.** (a) 300 × 300 Å$^2$ STM image of the mixed hex-$\sqrt{7} \times \sqrt{3}/2 \times 2$ surface acquired at RT. Inset shows a large-scale (4000 × 4000 Å$^2$) image of the surface where dark and bright regions correspond to $2 \times 2$ and hex-$\sqrt{7} \times \sqrt{3}$ domains, respectively. (b) 500 × 500 Å$^2$ STM image of a similar surface after it has transformed into $\sqrt{7} \times \sqrt{7}$ one upon cooling to 214 K. Regions of the remaining hex-$\sqrt{7} \times \sqrt{3}$ reconstruction are indicated as hex. Inset shows a FFT pattern taken from this surface. (c) and (d) LEED patterns taken from the mixed hex-$\sqrt{7} \times \sqrt{3}/2 \times 2$ surface at RT and 214 K, respectively. Dashed ovals in LEED pattern (d) and FFT pattern in inset in (b) indicate three reflections of which edge two correspond to $\sqrt{7} \times \sqrt{7}$ superstructure and the one in between is a sign of remaining $\sqrt{7} \times \sqrt{3}$ reconstruction. (e) Schematic LEED patterns of the $\sqrt{7} \times \sqrt{3}$, $2 \times 2$, and $\sqrt{7} \times \sqrt{7}$ superstructures with corresponding super-reflections shown by open red, yellow and green circles, respectively. They are also shown in the LEED patterns in (c) and (d) to guide an eye. In the schematic of the $\sqrt{7} \times \sqrt{3}$ superstructure reflections that are actually seen the LEED pattern are shown by filled red circles. (For interpretation of the references to color in this figure, the reader is referred to the web version of this article.)

random structure searching (AIRSS) method [19] which has already proven to be an efficient and effective method for exploring equilibrium structures of solids [20], point defects [21], surfaces [22,11,23], and clusters [24]. The In/Si(111)$\sqrt{7}\times\sqrt{7}$ supercell geometry was simulated by a repeating slab of four Si bilayers and a vacuum region of ~15 Å. Si atoms in the bottom one bilayer were fixed at their bulk positions, top three bilayers were allow to fully relax, and dangling bonds on the bottom surface were saturated by hydrogen atoms. The plane wave kinetic cutoff energy was 250 eV, and a Monkhorst-Pack 7 × 7 × 1 *k*-point mesh was used to sample the surface Brillouin zone within AIRSS. The geometry optimization is performed until the residual force was smaller than 5 meV/Å. Further tests on 400 eV energy cutoff show that the total energy is converged to with 1 meV per 1 × 1 unit cell.

## 3. Results and discussion

The first task to be solved in this study was to establish the In content in the In/Si(111)$\sqrt{7}\times\sqrt{7}$ phase. STM observations did not detect considerable mass transport during phase transition. Hence, the In coverage of the low-temperature phase is expected to be close to 1.2 ML, the In coverage of the room-temperature $\sqrt{7}\times\sqrt{3}$ phase. The most plausible candidates are 1.14 and 1.29 ML In, i.e., 8 and 9 In atoms per $\sqrt{7}\times\sqrt{7}$ unit cell. Seemingly, the problem can be resolved directly using STM observations just by measuring the change in the area fraction occupied by 2 × 2 or rec-$\sqrt{7}\times\sqrt{3}$ phases (which domains coexist with hex-$\sqrt{7}\times\sqrt{3}$) as a result of the transition. Note that 2 × 2 or rec-$\sqrt{7}\times\sqrt{3}$ phases are known to remain unchanged during cooling, at least, down to ~20 K [13]. Unfortunately, effects of the tip-induced electromigration are so substantial in the STM observations in the In/Si(111) system that apparent In coverage appears to be bias-dependent and to change in the course of recording successive images [13,25]. While acquiring filled-state STM images (i.e., with negative sample bias voltage) In atoms are repelled from the area under the tip apex but they are attracted there while acquiring empty-state images when the sample bias voltage is positive. All these hamper an accurate and reliable determination of In coverage in this system using STM. Therefore, we used LEED observations to reach the goal as this technique is free of the above side effects.

Design of the LEED experiment was as follows. The original In/Si(111) surface was prepared by depositing somewhat less than exactly 1.2 ML In, hence it contains coexisting regions of hex-$\sqrt{7}\times\sqrt{3}$ (1.2 ML In) and 2 × 2 (1.0 ML In) (Fig. 1a). This is reflected by the corresponding RT-LEED pattern which contains super-reflections from both, $\sqrt{7}\times\sqrt{3}$ and 2 × 2, reconstructions (Fig. 1c). One can note that the LEED pattern is rather faint. In case of the $\sqrt{7}\times\sqrt{3}$, this is a characteristic feature of its LEED pattern where only selected reflections of an ideal pattern (Fig. 1e) are seen [8]. The faint 2 × 2 spots are due to minor area fraction occupied by this phase. Then, the sample was cooled to 214 K. Two possible scenarios could be expected depending whether $\sqrt{7}\times\sqrt{7}$ phase contains more or less than 1.2 ML In of the hex-$\sqrt{7}\times\sqrt{3}$ phase. If it contains more than 1.2 ML In, then upon $\sqrt{7}\times\sqrt{3}$-to-$\sqrt{7}\times\sqrt{7}$ transition the area occupied by the $\sqrt{7}\times\sqrt{7}$ phase should be less than the area of the original hex-$\sqrt{7}\times\sqrt{7}$ phase. In this case the 2 × 2 domains would naturally increase in area (Remind that 2 × 2 is known to remain unchanged upon cooling). In the opposite case ($\sqrt{7}\times\sqrt{7}$ contains less than 1.2 ML In), excess In would be liberated upon transition. These liberated In atoms accumulating in the 2 × 2 regions would increase local In coverage there up to the value of $\sqrt{7}\times\sqrt{7}$ phase and induce its transformation to $\sqrt{7}\times\sqrt{7}$ phase. Thus, the 2 × 2 area would decrease and even disappear completely if its original area fraction was not large. This was exactly the case observed in the experiment. In the LEED pattern taken at 214 K (Fig. 1d) and showing $\sqrt{7}\times\sqrt{7}$ reflections, no 2 × 2 reflections are seen. However, one can notice also remaining faint $\sqrt{7}\times\sqrt{3}$ features (reflection in between two $\sqrt{7}\times\sqrt{7}$ reflections in the area indicated by the dashed oval in Fig. 1d). This is a sign of local areas near defects where the hex-$\sqrt{7}\times\sqrt{3}$ was preserved (see STM image with corresponding FFT pattern in Fig. 1b). In conclusion, results of LEED experiments have demonstrated that $\sqrt{7}\times\sqrt{7}$ phase contains less than 1.2 ML In, plausibly 1.14 ML (8 In atoms per $\sqrt{7}\times\sqrt{7}$ unit cell).

With the knowledge on plausible composition of the $\sqrt{7}\times\sqrt{7}$-In reconstruction, we applied the ab anitio random structure searching (AIRSS) technique to elucidate its atomic arrangement. The basic algorithm of the AIRSS method resides is random placing of a given number of certain atoms (here, eight In atoms) onto a given surface (here, unreconstructed Si(111) surface), after which the system is allowed to relax until it reaches a minimal formation energy. In general case, the latter corresponds to a certain local minimum. The procedure is repeated many times (in the present evaluation, 100 times) and the structures are ranked in accordance with their formation energies. Typically, the corresponding graph shows up as a set of distinct horizontal plateaus corresponding to local minima of which the lowest plateau shows the promise for reaching the global minimum. In the present case of evaluation for $\sqrt{7}\times\sqrt{7}$-In structure the graph has an unusual shape (Fig. 2). Instead of the distinct plateaus there is a set of about 55 structures having very close formation energies. Their deviations from each other are within only ~5 meV per 1 × 1 cell.

A close look on the atomic structures constituting the above set allows us to subdivide them into the three main groups labeled A, B, and C in Fig. 3. The groups represent qualitatively different structures. In particular, the structures belonging to the A group can be visualized as two-atom-wide meandering chains interconnected to each other with a $\sqrt{7}$ periodicity. Note that in the A structures all In atoms occupy non-regular adsorption sites (i.e., neither $T_4$, nor $H_3$, nor $T_1$).

In the C structures all In atoms within the $\sqrt{7}\times\sqrt{7}$ unit cell also reside in non-regular sites except for the one In atom that occupies the $T_4$ site. The C structures (as well as the B ones) show up as flexible two-dimensional atomic networks. Characteristic feature of the C structures is occurrence of the relatively large holes centered in the $H_3$ site and having a shape of irregular hexagon within atomic array. The C structure can also be visualized as interconnected two-atom-wide chains aligned along the three $\sqrt{7}$ directions.

In contrast to A and C structures, the B structure is the only one that reproduces the $C_3$ symmetry of the Si(111) surface. The basic structure (labeled B1) incorporates within each $\sqrt{7}\times\sqrt{7}$ unit cell one In atom in the $T_1$ site, four In atoms in the $T_4$ sites and the other three In atoms occupying non-regular sites. Of the four $T_4$ In atoms, three atoms form a kind of trimer and the other can be considered as an adatom. Upon transformation successively to the B2 and B3 structures the In trimer increases in size, that forces the $T_1$ and $T_4$ In adatoms to leave their regular

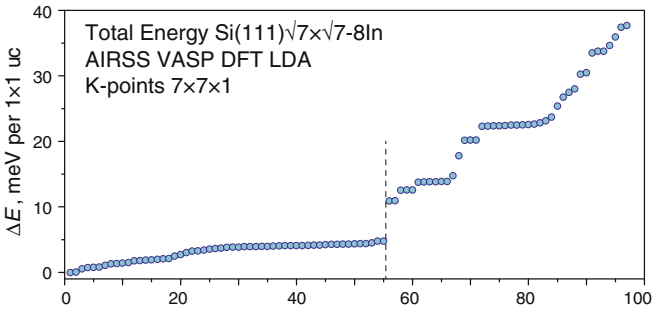


**Fig. 2.** Results of the AIRSS analysis of the structural models with 8 In atoms per $\sqrt{7}\times\sqrt{7}$ unit cell. Models are ranked in accordance with their total energies (referred to the lowest energy structure). The models to the left from the vertical dashed line have very close formation energies.

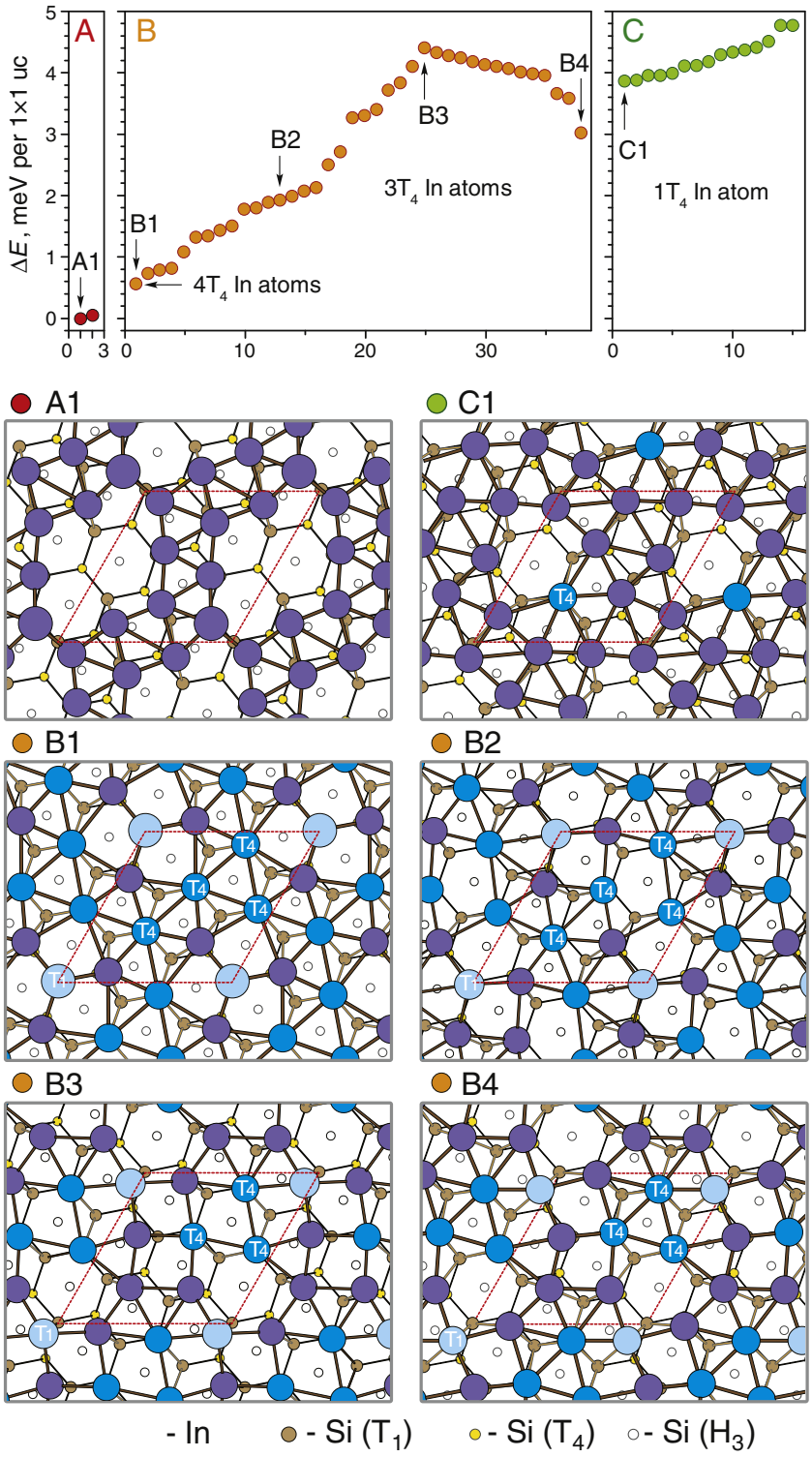


**Fig. 3.** Upper panel: Subdivision of the first 55 lowest-energy models into three groups, A, B, and C. The group B is subdivided further into the models B1, B2, B3, and B4. Lower panel: atomic arrangement of the models belonging to the various groups. In atoms occupying $T_4$ sites are shown by bright blue circles, In atoms occupying on-top ($T_1$) sites by light blue circles, In atoms occupying random non-regular sites by dark blue circles. Si atoms are shown by brown circles (for $T_1$ sites), yellow circles (for $T_4$ sites), and white circles for ($H_3$ sites). The $\sqrt{7} \times \sqrt{7}$ unit cell is outlined by the red line. (For interpretation of the references to color in this figure, the reader is referred to the web version of this article.)

sites (without forming a trimer). In the final B4 structure three In atoms (making a trimer) reside in the $T_4$ sites while the other five In atoms are in non-regular sites. One can also note developing of the hexagonal holes within atomic array. Fig. 4 illustrates trajectories of atomic displacements of all In atoms within $\sqrt{7} \times \sqrt{7}$ unit cell in the course of B1 → B2 → B3 → B4 transformations.

Fig. 5 shows simulated STM images for the overall set of the structural models. In order to clarify the origin of the observed STM features, the

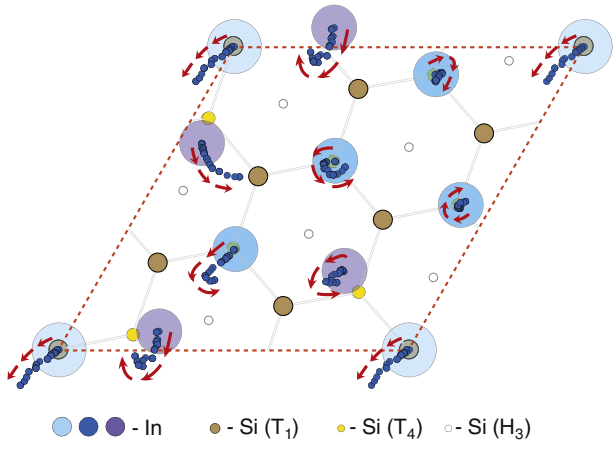


**Fig. 4.** Trajectories of the shifting In atoms constituting the $\sqrt{7} \times \sqrt{7}$ B structures in the course of B1 → B2 → B3 → B4 transformations. The large faint circles correspond to In atom location in the B1 structure (see Fig. 3). Small circles show transient atom positions. Red arrows indicate the direction of atom shifts. In and Si atoms are shown by the circles of the same color as in Fig. 3. (For interpretation of the references to color in this figure, the reader is referred to the web version of this article.)

basic fragments of the structural models are superposed onto the STM images. One can notice a considerable variance in STM appearance of different structures. Thus, bearing in mind that all the structures have a very close formation energy, one could expect that experimental STM images have to display rather heterogeneous surface patterns with patches having various STM appearance. In reality, the experimental STM images do confirm the principal expectations based on the AIRSS results. As an example, STM image in Fig. 6a provides an indication on the flexibility of the $\sqrt{7} \times \sqrt{7}$-In layer which is continuously changing its structure during scanning. In particular, one can see that the patches of the surface structure having $C_3$ symmetry can gradually transform into those with $C_1$ symmetry and vice versa. Definite changes in STM appearance of the In/Si(111) layer can be seen around surface defects and in the regions where doubling of the $\sqrt{7}$ periodicity spontaneously occurs (see Fig. 6b). Note that occurrence of $2\sqrt{7} \times \sqrt{7}$ superstructure (as well as other long-periodic structures [13]) indicates the possibility of the formation of the phases with multiple $\sqrt{7}$ periodicities. Nevertheless, they are closely related to the basic $\sqrt{7} \times \sqrt{7}$ structure. A close look on the experimental STM images (e.g., as in Fig. 6b) allows us to find there the counterparts of the simulated STM images of Fig. 5. The corresponding plausible structures are indicated. However, it is worth noting that this correspondence is not complete. Namely, the counterparts of some model structures (e.g., A1, B1, B2) are lacking. Among them, the absence of A1-like features seems to be the most unexpected, since the A1 structure has the lowest formation energy. The possible reason might be related to the certain kinetic limitations that are not considered in AIRSS.

## 4. Conclusion

Upon cooling the atom-layer-thick In/Si(111) interface, the hex-$\sqrt{7} \times \sqrt{3}$ surface reconstruction undergoes a reversible transition to the $\sqrt{7} \times \sqrt{7}$ structure. As revealed by the LEED observations, the transition is accompanied by loosing certain portion of In. While the room-temperature hex-$\sqrt{7} \times \sqrt{7}$-In reconstruction contains 1.2 ML In, the low-temperature $\sqrt{7} \times \sqrt{7}$-In phase incorporates plausibly eight In atoms per $\sqrt{7} \times \sqrt{7}$ unit cell, i.e. ~1.14 ML In. Using this data on $\sqrt{7} \times \sqrt{7}$-In composition, we have applied AIRSS technique to elucidate its structure. However, instead of a well-defined single lowest-energy

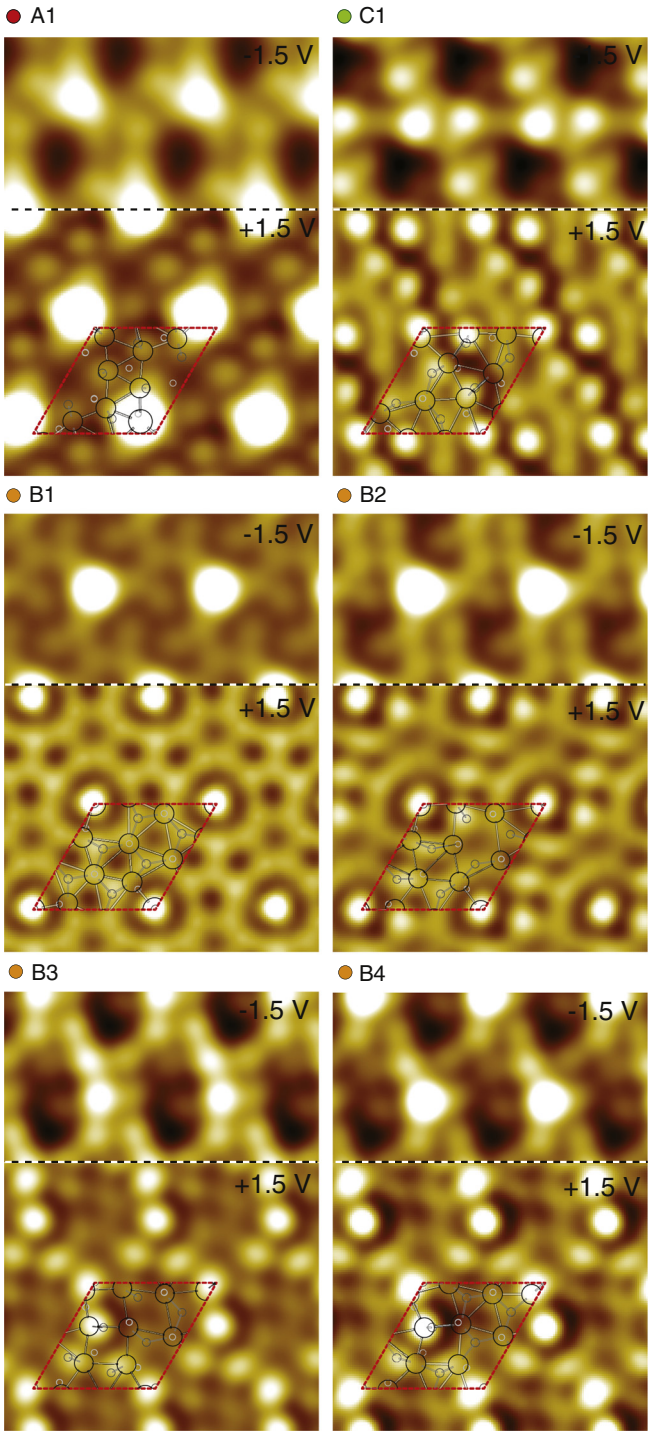


**Fig. 5.** Simulated dual-polarity (±1.5 V) STM images for the basic structural models. The $\sqrt{7} \times \sqrt{7}$ unit cell is outlined by the red line. Corresponding fragments of the structural models are superposed on the images to illustrate the origin of the STM features. (For interpretation of the references to color in this figure, the reader is referred to the web version of this article.)

structure, the AIRSS demonstrates occurrence of a set of various surface structures having very similar formation energies. Indeed, STM observations reveal that a flexible In layer contains patches with various STM appearance that gradually transform from one to another. Some of the model structures (albeit not all) have their counterparts in the experimental STM images.

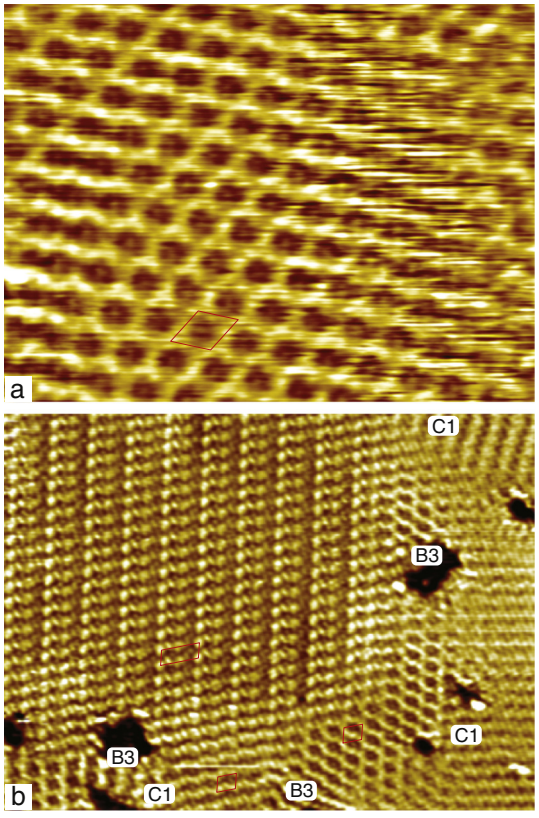


**Fig. 6.** (a) Empty-state (+1.5 V) 130 × 100 Å$^2$ and (b) filled-state (−1.5 V) 275 × 210 Å$^2$ experimental STM images of the Si(111)$\sqrt{7} \times \sqrt{7}$-In surface. The regions which represent plausibly the counterparts of the model structures are indicated. Unit cells of the $\sqrt{7} \times \sqrt{7}$ and $2\sqrt{7} \times \sqrt{7}$ are outlined by red parallelograms. (For interpretation of the references to color in this figure, the reader is referred to the web version of this article.)

## Acknowledgements

The work was supported in part by Russian Foundation for Basic Researches through Grant No. 14-02-92001, by Russia President Grant No. MK-6592.2015.2 for young researches, by the RAS "Far East" Program Grant No 0262-2015-055, by Ministry of Science and Technology of Taiwan through Grant No. 103-2923-M-001-005-MY3 and by the Supercomputing Center of Lomonosov Moscow State University.

## References

[1] T. Zhang, P. Cheng, W.J. Li, Y.J. Sun, G. Wang, X.G. Zhu, K. He, L. Wang, X. Ma, X. Chen, Y. Wang, Y. Liu, H.Q. Lin, J.F. Jia, Q.K. Xue, Nat. Phys. 6 (2010) 104.
[2] T. Uchihashi, P. Mishra, M. Aono, T. Nakayama, Phys. Rev. Lett. 107 (2011) 207001.
[3] M. Yamada, T. Hirahara, S. Hasegawa, Phys. Rev. Lett. 110 (2013) 237001.
[4] J. Noffsinger, M.L. Cohen, Solid State Commun. 151 (2011) 421.
[5] S.H. Uhm, H.W. Yeom, Phys. Rev. B 86 (2012) 245408.
[6] T. Uchihashi, P. Mishra, T. Nakayama, Nanoscale Res. Lett. 8 (2013) 167.
[7] C. Brun, T. Cren, V. Cherkez, F. Debontridder, S. Pons, D. Fokin, M.C. Tringides, S. Bozhko, L.B. Ioffe, B.L. Altshuler, D. Roditchev, Nat. Phys. 10 (2014) 444.
[8] J. Kraft, S.L. Surnev, F.P. Netzer, Surf. Sci. 340 (1995) 36.
[9] J.W. Park, M.H. Kang, Phys. Rev. Lett. 109 (2012) 166102.
[10] K. Uchida, A. Oshiyama, Phys. Rev. B 87 (2013) 165433.
[11] J.P. Chou, C.M. Wei, Y.L. Wang, D.V. Gruznev, L.V. Bondarenko, A.V. Matetskiy, A.Y. Tupchaya, A.V. Zotov, A.A. Saranin, Phys. Rev. B 89 (2014) 155310.
[12] S.G. Kwon, M.H. Kang, Phys. Rev. B 89 (2014) 165304.
[13] A.A. Saranin, A.V. Zotov, M. Kishida, Y. Murata, S. Honda, M. Katayama, K. Oura, D.V. Gruznev, A. Visikovskiy, H. Tochihara, Phys. Rev. B 74 (2006) 035436.
[14] P.E. Blöchl, Phys. Rev. B 50 (1994) 17953.
[15] G. Kresse, D. Joubert, Phys. Rev. B 59 (1999) 1758.
[16] G. Kresse, J. Hafner, Phys. Rev. B B49 (1994) 14251.
[17] G. Kresse, J. Furthmüller, Comput. Mater. Sci. 6 (1996) 15.
[18] D.M. Ceperley, B.J. Alder, Phys. Rev. Lett. 45 (1980) 566.
[19] C.J. Pickard, R.J. Needs, J. Phys. Condens. Matter 23 (2011) 053201.
[20] C.J. Pickard, R.J. Needs, Phys. Rev. Lett. 97 (2006) 045504.
[21] A.J. Morris, C.J. Pickard, R.J. Needs, Phys. Rev. B 78 (2008) 184102.
[22] D. Gruznev, A. Matetskiy, L. Bondarenko, O. Utas, A. Zotov, A. Saranin, J. Chou, C. Wei, M. Lai, Y. Wang, Nat. Commun. 4 (2013) 1679.
[23] D.V. Gruznev, L.V. Bondarenko, A.V. Matetskiy, A.Y. Tupchaya, A.A. Alekseev, C.R. Hsing, C.M. Wei, S.V. Eremeev, A.V. Zotov, A.A. Saranin, Phys. Rev. B 91 (2015) 035421.
[24] J.P. Chou, C.R. Hsing, C.M. Wei, C. Cheng, C.M. Chang, J. Phys. Condens. Matter 25 (2013) 125305.
[25] A.A. Saranin, T. Numata, O. Kubo, H. Tani, M. Katayama, V.G. Lifshits, K. Oura, Phys. Rev. B 56 (1997) 7449.